NIH Public Access
Author Manuscript
Anal Chem. Author manuscript; available in PMC 2013 November 20.

Published in final edited form as:
Anal Chem. 2012 November 20; 84(22): 9935–9941. doi:10.1021/ac302347y.

Utilizing a Water-Soluble Cryptophane with Fast Xenon Exchange Rates for Picomolar Sensitivity NMR Measurements

Yubin Bai, **P. Aru Hill**[†], and **Ivan J. Dmochowski**[*]
Department of Chemistry, University of Pennsylvania, Philadelphia, Pennsylvania 19104

Abstract

Hyperpolarized ^{129}Xe chemical exchange saturation transfer (^{129}Xe Hyper-CEST) NMR is a powerful technique for the ultrasensitive, indirect detection of Xe host molecules (e.g., cryptophane-A). Irradiation at the appropriate Xe-cryptophane resonant radio frequency results in relaxation of the bound hyperpolarized ^{129}Xe and rapid accumulation of depolarized ^{129}Xe in bulk solution. The cryptophane effectively 'catalyzes' this process by providing a unique molecular environment for spin depolarization to occur, while allowing xenon exchange with the bulk solution during the hyperpolarized lifetime ($T_1 \approx 1$ min). Following this scheme, a triacetic acid cryptophane-A derivative (TAAC) was indirectly detected at 1.4 picomolar concentration at 320 K in aqueous solution, which is the record for a single-unit xenon host. To investigate this sensitivity enhancement, the xenon binding kinetics of TAAC in water was studied by NMR exchange lifetime measurement. At 297 K, $k_{on} \approx 1.5 \times 10^6$ $M^{-1}s^{-1}$ and $k_{off} = 45$ s^{-1}, which represent the fastest Xe association and dissociation rates measured for a high-affinity, water-soluble xenon host molecule near rt. NMR linewidth measurements provided similar exchange rates at rt, which we assign to solvent-Xe exchange in TAAC. At 320 K, k_{off} was estimated to be 1.1×10^3 s^{-1}. In Hyper-CEST NMR experiments, the rate of ^{129}Xe depolarization achieved by 14 pM TAAC in the presence of RF pulses was calculated to be 0.17 $\mu M \cdot s^{-1}$. On a per cryptophane basis, this equates to 1.2×10^4 ^{129}Xe atoms s^{-1} (or 4.6×10^4 Xe atoms s^{-1}, all Xe isotopes), which is more than an order of magnitude faster than k_{off}, the directly measurable Xe-TAAC exchange rate. This compels us to consider multiple Xe exchange processes for cryptophane-mediated bulk ^{129}Xe depolarization, which provide at least 10^7-fold sensitivity enhancements over directly detected hyperpolarized ^{129}Xe NMR signals.

Keywords

Hyper-CEST; ^{129}Xe Hyperpolarization; Chemical Exchange Saturation Transfer; Biosensor

INTRODUCTION

Methods for detecting trace analytes play critical roles in chemistry and many applied fields, including biotechnology, biophysics, molecular pathology, metallurgy and homeland security. Nuclear magnetic resonance (NMR) spectroscopy is a versatile technique for probing molecular structure but typically offers limited detection sensitivity, based on the small magnetic moment of commonly employed nuclei (e.g., ^{1}H, ^{13}C, ^{15}N) and the narrow

[*]**Corresponding Author**ivandmo@sas.upenn.edu.
[†]Present Addresses Schmahl Science Workshops, San Jose, California 95112.

SUPPORTING INFORMATION
HP Xe delivery setup, ITC controls at 310 K, and detailed kinetic model. This material is available free of charge via Internet at http://pubs.acs.org.

separation in energy levels between nuclear spin transitions. This leads to small polarization of the nuclear spin reservoir, where the difference in spin populations aligned parallel or anti-parallel to an external magnetic field at thermal equilibrium is typically just 1 in ~10^5 spins. Thus, significantly enhanced NMR signals can be obtained via hyperpolarization techniques capable of generating a nuclear spin polarization level approaching 100%.[1,2]

For applications in biodetection and materials science, we[3–6] and others[7–20] have investigated the noble gas isotope ^{129}Xe, which is spin-½ and readily hyperpolarized (HP) via spin-exchange optical pumping.[2,21] However, due to low concentrations of the delivered magnetic species and short spin relaxation lifetimes, the signal intensity is still not ideal for many demanding applications, e.g., clinical MRI.[22,23] When exchanging magnetic species are present, chemical exchange saturation transfer (CEST) can provide another source of signal amplification based on cumulative magnetization transfer through selective saturation.[24] For proton MRI, CEST contrast originates from exchange of endogenous or exogenous amide or hydroxyl protons with bulk water protons, or from exchangeable sites on paramagnetic inorganic coordination complexes.[25,26] This gives the possibility of designing extremely sensitive contrast agents that respond to various exchange events, with techniques known as PARACEST[27] and LIPOCEST.[28] More recently, the analogous technique involving HP ^{129}Xe CEST (Hyper-CEST) was developed.[8] Based on its considerable polarizability, xenon exhibits significant affinity for organic host molecules known as cryptophanes.[4–6,10,29–32] In one example, Hyper-CEST was applied to virus capsids modified by ~125 cryptophanes, thereby attaining 0.7 pM capsid detection sensitivity.[15]

Here we present ultrasensitive Hyper-CEST NMR with a water-soluble triacetic acid cryptophane-A derivative (TAAC, Figure 1).[5] ^{129}Xe NMR biosensors using similarly derivatized cryptophanes have been shown previously to be useful for detecting a wide variety of analytes.[3,7,12,33–39] This single-unit cryptophane derivative, TAAC, was indirectly detected at 1.4 picomolar concentration at 320 K in aqueous solution, which is the record for a xenon host. Thermodynamic and kinetic studies of xenon binding were carried out to investigate this sensitivity enhancement, which establish TAAC as a very effective xenon binder/'spin catalyst' under the Hyper-CEST scheme. Our results suggest multiple Xe exchange processes for cryptophane-mediated HP ^{129}Xe NMR signal enhancement.

EXPERIMENTAL

Materials

TAAC was previously prepared by a thirteen-step synthesis,[5] and found to be soluble to ~500 μM in aqueous solution (pH 7), owing to its three carboxylates. The identity and purity of TAAC were confirmed by ^{1}H NMR spectroscopy. TAAC features a xenon association constant (K_A) of 33 000 M^{-1} at 293 K, making it currently one of the highest-affinity Xe host molecules.[5,6,31]

Ultra-filtered water (18 MΩ·cm resistivity) obtained from Mar Cor filtration system, was used to prepare TAAC solutions. TAAC (1.43 mg) was carefully weighed and dissolved in 10 mL water to form a 140 μM solution, which was confirmed by Agilent 8453 UV-vis spectrophotometer (ε_{280} = 12 000 $M^{-1}cm^{-1}$). For the Hyper-CEST experiments a series of 10-fold dilutions with ultra-filtered water was performed to bring TAAC solution down to picomolar concentrations. Dilutions were made with well calibrated Eppendorf Research pipettes with <1% error. After each dilution, solution was vortexed to homogenize sample. Reagents were used as purchased from Fisher: sodium phosphate dibasic heptahydrate, sodium phosphate monobasic dihydrate. Prior to isothermal titration calorimetry (ITC)

measurement, TAAC solution was dialyzed in phosphate buffer (20 mM, pH 7.5) by GE Mini Dialysis Kit (1 kDa cut-off).

In the NMR samples, xenon concentrations were calculated by multiplying the xenon partial pressure with its mole-fraction solubility in water, at a given temperature. For example, during the Hyper-CEST experiment at 320 K, [Xe, all isotopes] is calculated as: xenon partial pressure in gas line × mole fraction solubility (at 320 K, 1 atm) × molarity of water = $0.045 \times 4.95 \times 10^{-5} \times 55.5$ M = 0.12 mM, following Henry's Law. The concentration of hyperpolarized ^{129}Xe in solution (3.1–4.8 μM) was determined by multiplying [Xe] by the natural isotopic abundance (26.4%) and the hyperpolarization level (10–15%), measured by comparing with thermal Xe sample.[40]

General NMR method

A 500 MHz Bruker BioDRX NMR spectrometer was used for all ^{129}Xe NMR measurements. RF pulse frequency for ^{129}Xe was 138.12 MHz. Samples were observed using either a 5 mm PABBO NMR probe or a similar 10 mm probe. HP ^{129}Xe was generated using a home-built ^{129}Xe hyperpolarizer, based on the Nycomed-Amersham (now GE) IGI.Xe.2000 commercial system. A gas mixture of 89% nitrogen, 10% helium, and 1% natural abundance xenon (Concord Gases, NJ) was used for the hyperpolarizer input. ^{129}Xe was hyperpolarized to 10–15% after optical pumping of Rb vapor with 795 nm circularly polarized laser, cryogenic separation of Xe, and accumulation and collection in CAV NMR tubes (New Era). For the TAAC spectrum and exchange rate measurements, after introducing HP Xe to sample solution, the sealed NMR tube was shaken vigorously to mix solution with HP ^{129}Xe.

Directly recorded ^{129}Xe NMR spectra were acquired using 30° hard excitation pulses (7.5 μs on 5 mm probe), or 90° EBurp1 shaped pulses (7.5 ms, 602 Hz excitation bandwidth). Spectra were signal averaged by 10–30 scans. A delay of 0.15 s was given between scans to allow depolarized Xe to leave the cryptophane cavity and fresh HP Xe to enter the cavity. The spectra shown in Figure 2 were exponentially broadened by 4 Hz to give a larger signal/noise ratio. Sample temperature was controlled by VT unit on NMR spectrometer to ± 1 K.

At a series of temperatures from 300–325 K, HP ^{129}Xe NMR spectra were acquired following the aforementioned protocol and the natural line widths of the Xe@TAAC peaks were fitted (FWHM, Lorentzian) and summarized in Table 1.

Hyper-CEST method

Scheme 1 illustrates the Hyper-CEST experiment involving TAAC. Before starting the pulse sequence each time, a controllable amount of HP Xe was delivered into the 3-mL sample solution, and sealed in the NMR tube for signal stabilization by a homebuilt continuous-flow HP Xe delivery setup (Figure S1). Multiple selective 180-degree radiofrequency (RF) pulses were delivered to the sample at the ^{129}Xe@TAAC resonance frequency, while HP Xe and depolarized Xe were dynamically exchanging in and out of TAAC. As a result, depolarized Xe was accumulated in the aqueous sample, and detected by another 90 degree hard excitation pulse. HP Xe in water undergoes depolarization exponentially by the time constant $T_1 \approx 70$ s. However, in the Hyper-CEST experiment TAAC served as a "depolarization catalyst", and could be turned "on" and "off" using a saturation frequency that was either on- or off-resonance with ^{129}Xe@TAAC.

Utilizing a home-built continuous flow HP Xe delivery setup (Supporting Information, Figure S1), freshly hyperpolarized Xe gas mixture was bubbled through sample solutions at 65 psi. Before starting the pulse program each time, bubbling was stopped by two solenoid valves to maintain magnetic field homogeneity.

The Hyper-CEST experiment was carried out using the pulse program illustrated in Figure 3. DSnob-shaped pulses (parameter sp6) were looped numerous times (L6) to induce xenon polarization transfer. In the low concentration trials, where d12 << sp6 in duration, the radiation became near-continuous. The DSnob pulse power was calibrated to give maximum saturation. With a single DSnob pulse (sp6) irradiated at Xe(aq) frequency, >90% signal was saturated. After the overall polarization was reduced by saturation pulses and chemical exchange, the sample was irradiated with a 90 degree hard pulse to read out the final magnetization state of ^{129}Xe in solution. Due to imperfection of frequency selectivity, sp6 contributed significantly to the off-resonance regions of the spectrum after 10 000 repeats. Therefore, for the lowest concentration TAAC Hyper-CEST experiments the Xe(aq) peaks were relaxed faster than the analogous T_1 of HP ^{129}Xe in aqueous solution.

Isothermal titration calorimetry (ITC)

ITC samples were prepared as described, and xenon binding measurements were performed using a MicroCal VP-ITC titration microcalorimeter (Northampton, MA) at 310 K. Standard protocols and data analyses were used. Control enthalpograms for ITC are presented in the Supporting Information (Figure S2– S4).

Xe@TAAC NMR line widths at different temperatures

The spectra were Lorentzian deconvolved to fit for full width at half maximum (FWHM). Peak widths of the Xe@TAAC peaks were corrected by subtracting the Xe(aq) peak line widths to account for magnet inhomogeneity. The line widths of Xe(aq) peaks range between 8–18 Hz (from 297 K to 320 K), which mainly originates from magnetic field homogeneity. This response of aqueous ^{129}Xe to temperature change was negligible compared to ^{129}Xe@TAAC peaks (Table 1).

Xenon exchange lifetime measurement

Though 2D EXSY NMR is the standard method for determining exchange rates,[41] selective 1D EXSY NMR[42–44] serves as a better measurement scheme in this case, due to the spectral dominance of the HP ^{129}Xe(aq) peak. Using a customized EXSY pulse sequence,[43] the Xe@TAAC resonance was selectively excited and acquired twice (separated by designated mixing times), generating two FIDs (initial and recovery). The ratio of signal intensities was calculated to quantify the percentage of Xe@TAAC replenishment, at a manually set mixing time that's close to the xenon exchange lifetime being fitted. With a series of exchange-replenishment ratios and their corresponding mixing times, Xe exchange lifetime can be fitted, providing a measurement of cryptophane-Xe exchange performance.

RESULTS AND DISCUSSION

Hyperpolarized ^{129}Xe NMR spectra of TAAC in aqueous solution

Two peaks arise in the HP ^{129}Xe NMR spectrum of 140 μM TAAC aqueous solution (Figure 2): Xe dissolved in water at 320 K (Xe(aq), 194.3 ppm) and Xe bound in TAAC (Xe@TAAC, 65.8 ppm). In HP ^{129}Xe detection schemes investigated to date, there is a large excess of Xe (mM) relative to cryptophane (μM),[45] which results in a Xe(aq) peak that is ~1000 times stronger than Xe@TAAC without selective excitation. Given the almost 130 ppm separation of the two peaks, selective RF pulses focused on Xe@TAAC will have little effect on Xe(aq) under most conditions, which allows selective excitation of the minor "cryptophane-bound" species as well as selective saturation exchange experiments.

Direct detection, even selective excitation (for example, Figure 2), requires micromolar cryptophane, which limits cryptophane biosensor experiments to prevalent biological targets. Some cryptophanes may also be toxic to cells at this concentration.[39,46] Instead of

trying to detect directly the ^{129}Xe@TAAC peak, the ^{129}Xe@TAAC resonance can be indirectly measured more sensitively via magnetization transfer from the much stronger ^{129}Xe(aq) NMR signal.

Xenon binding kinetics of TAAC

The thermodynamics of xenon binding is established by the equilibrium shown in eq 1:

$$\mathrm{Xe+S@TAAC} \underset{k'_{off}}{\overset{k_{on}}{\rightleftharpoons}} \mathrm{Xe@TAAC+S} \quad (1)$$

where S@TAAC indicates solvent-bound TAAC. It is experimentally observed[47] that "empty" cryptophane is preferably bound with solvent, in this case one or multiple water molecules. Because the concentration of solvent is constant, the reverse process in eq 1 can be simplified to be first-order, yielding the rate constant 'k_{off}' (k'_{off}[S]). This yields eq 2 with the rate constants of xenon binding (k_{on}) and dissociation (k_{off}) indicated:

$$k_{on}[\mathrm{Xe}][\mathrm{S@TAAC}] = k_{off}[\mathrm{Xe@TAAC}] \quad (2)$$

The maximal Hyper-CEST effect should occur under conditions where all of the cryptophane is encapsulating xenon (to ensure maximal Xe absorption of the RF pulse) while still allowing the most rapid "Xe in"-"Xe out" exchange. The xenon on- and off-rates (k_{on}, k_{off}) describe the rates at which HP Xe gains access to the cavity of TAAC and the rate at which depolarized Xe leaves TAAC. This exchange process should occur most rapidly when a HP Xe atom directly displaces depolarized Xe, with no intermediary solvent binding. However, because TAAC experiments are conducted in water, solvent may compete with Xe binding.

Ultrasensitive detection of TAAC

Picomolar TAAC was detected by a series of Hyper-CEST measurements, following the general method developed in the Pines lab.[15] In Figure 4, relative intensity of Xe(aq) signal was plotted against the time of saturation transfer pulse cycles. As in Figure 3, the shaped saturation pulse was configured to resonate at the frequency of Xe@TAAC signal (65.8 ppm). As a control, saturation at a mirror frequency (2 × 194.3 – 65.8 = 322.8 ppm) was established, to perform off-resonance Hyper-CEST. When the saturation pulse was tuned to Xe(aq) frequency, the peak was able to be completely saturated with 2 scans. At 14 pM TAAC concentration and higher, on-resonance Hyper-CEST clearly presented a more sharply decaying Xe depolarization curve, indicating effective saturation transfer. After 10-fold dilution, the difference in depolarization rate was still observable from exponential fits; representative data from three trials are shown. Detection of 1.4 pM TAAC is currently the lowest observed concentration for a single-unit Xe host. Previously, the Pines lab demonstrated detection of 10 nM cryptophane using this technique.[48] To explain the much greater detection sensitivity obtained in the current experiment, we hypothesized that TAAC must have much more rapid xenon exchange kinetics compared to previously measured cryptophane systems, in addition to its favorably high Xe@TAAC occupancy. To explore the origins of the achieved sensitivity, a series of characterization experiments was performed.

ITC measurement of xenon binding to TAAC

TAAC should be favorable for Hyper-CEST NMR based on its high Xe affinity. Moreover, its strongly positive entropy of Xe binding (ΔS = 5.9 cal·mol^{-1}·K^{-1} at 293 K) supports high affinity as temperature increases from rt to physiological conditions.[5] Indeed, ITC

measurements performed at 310 K showed the Xe-TAAC association constant to be 33 000 ± 2000 M^{-1} (Figure 5), the same value determined at 293 K.[5] During the Hyper-CEST experiment, xenon concentration[45] is calculated to be 0.12 mM by assuming the hyperpolarized Xe gas mixture, at 1 atm, saturates the sample solution. Therefore, more than 80% of the TAAC molecules were bound to Xe, which is higher than the 45–60% host occupancy in previous Hyper-CEST NMR experiments.[15,20,48]

Xe@TAAC NMR line widths at different temperatures

Spectra were acquired for 140 μM TAAC aqueous solution following the same method as Figure 2, at different temperatures (see Table 1). The spectra were Lorentzian deconvolved to fit for full width at half maximum (FWHM). Peak widths of the Xe@TAAC peaks were corrected by subtracting the Xe(aq) peak line widths to account for magnet inhomogeneity.

Xenon exchange lifetime measurement

Previously, Xe-cryptophane exchange rates in organic solution were measured by 2D ^{129}Xe NMR[42] spectroscopy and approximated by measuring the line width of the Xe@cryptophane NMR resonance.[29] Due to the high concentrations of xenon and cryptophane that dissolved in $C_2D_2Cl_4$,[42] it was possible to use the small ^{129}Xe polarization provided by the NMR magnet. Here, in order to examine the origins of the heightened cryptophane-mediated HP ^{129}Xe depolarization achieved with TAAC, we sought to measure the xenon-cryptophane exchange kinetics in aqueous solution by the combination of NMR selective excitation and ^{129}Xe hyperpolarization, which was demonstrated previously for a biotin-derivatized xenon biosensor.[43]

By altering the exchange mixing time, a series of Xe replenishment efficiencies was measured (Figure 6). The xenon exchange lifetime, τ_{exch}, was determined to be 22 ± 3 ms at 297 K. This τ_{exch} value is shorter than measured for all previous cryptophanes in water close to rt.[31,32,43,49] Using the measured τ_{exch} and K_A, xenon dissociation and association rate constants were determined at 297 K: $k_{off} \approx k_{exch} = 1/\tau_{exch} = 45 \pm 15\ s^{-1}$ and $k_{on} \approx 1.5 \times 10^6\ M^{-1}s^{-1}$. As k_{exch} is an intermolecular process,[29] it likely underestimates the Xe dissocation rate (k_{off}).[43] Despite this difference, the measured rates are more than 2-fold faster than the exchange rates measured for water-soluble cryptophanes with comparable Xe affinity ($k_{on} = 3.8 \times 10^5\ M^{-1}s^{-1}$; $k_{off} = 13.1\ s^{-1}$ at 293 K[31,32]). Our measured exchange rates with TAAC in water are more typical of cryptophane-A derivatives in organic solvent, where millisecond timescales have been observed.[29] A key difference, however, is that in large organic solvents such as $C_2D_2Cl_4$, the cryptophane should remain empty during the Xe exchange process. In water, solvent binding to TAAC will slow the Xe exchange process.

It has been established by Pines and co-workers that Hyper-CEST becomes dramatically more sensitive at temperatures slightly above rt,[48] but the origin of this effect requires further investigation. Using our experimental setup, we were unable to measure the exchange rate ($1/\tau_{exch}$) exactly at 320 K, where the Hyper-CEST experiment was performed. However, HP ^{129}Xe NMR spectra collected at different temperatures (Table 1) provide estimates for k_{exch} from Xe@TAAC peak line widths: $k_{exch} = 1100\ s^{-1}$ at 320 K, $k_{exch} = 500\ s^{-1}$ at 310 K, $k_{exch} = 86\ s^{-1}$ at 300 K, which is in reasonable agreement with the 1-D EXSY exchange rate measurement at 297 K ($k_{exch} = 45\ s^{-1}$). For the ~20% water-bound TAAC in solution, the exchange rate should be limited by the dissociation of water en route to Xe binding.

Description of HP Xe depolarization rate

In the overall depolarization “reaction” resulting in thermal equilibration of all xenon nuclear spins in solution, TAAC (together with selective saturation RF pulses) acts as a ‘spin

catalyst'. Depolarization curves were fit using first-order kinetics, with the TAAC-mediated HP Xe depolarization rate constant (k_{TAAC}) and the natural T_1 relaxation rate constant (k_1) both contributing to the observed loss of HP Xe (Supporting Information). By multiplying k_{TAAC} by the starting HP Xe concentration (3.1 μM), the maximum HP Xe depolarization rate can be expressed as k_{TAAC}·[HP Xe] = 0.17 μM·s^{-1}. After dividing by TAAC concentration (14 pM), this equates to $k_{cat} = 1.2 \times 10^4$ HP Xe-129 atoms depolarized by each TAAC molecule per second. Compared to a virus-capsid-based biosensor which we calculate to have $k_{cat} = 1.3 \times 10^2$ s^{-1},[15] TAAC is observed to have 100-times greater activity on a per-cryptophane basis (Supporting Information).

For TAAC, which is ~80% bound with Xe in solution, the Xe-Xe exchange rate, $k_{exch(Xe\text{-}Xe)}$, should be the critical kinetic parameter for determining Hyper-CEST efficiency. Based on very efficient saturation transfer (> 0.9 in a control experiment), we assume in our analysis of TAAC that k_{cat} approximates the Xe-Xe exchange rate. Including all Xe isotopes, $k_{exch(Xe\text{-}Xe)}$ should be approximately $k_{cat}/0.26 = 4.6 \times 10^4$ s^{-1}. At 320 K this is more than one order of magnitude faster than k_{off}, the proposed Xe-H_2O exchange rate measured by NMR linewidth. This suggests that there are two different kinetic processes, with only the slower H_2O-Xe exchange process being directly observable by either 1-D EXSY or NMR linewidth measurements. Such millisecond exchange processes are most consistent with previously published Hyper-CEST NMR results,[8,15,20,36] which led to detection of nanomolar cryptophane concentrations.

Some of TAAC's advantage in a Hyper-CEST detection scheme may arise from differences in cryptophane solubilization; for example, TAAC's three acetates should promote more open, Xe-accessible conformations of the cryptophane, with high xenon on- and off-rates.[47] Our previous fluorescence lifetime studies indicated that only 5–10% of TAAC in aqueous solution adopts a more collapsed, non-Xe binding conformation.[5] In addition, high Xe occupancy and narrower line widths for the HP ^{129}Xe-cryptophane complex promote RF saturation leading to efficient HP ^{129}Xe depolarization.

Depolarization mechanisms

Multiple processes may contribute to rapid Xe depolarization, beyond the discussed Hyper-CEST Xe-cryptophane-water exchange mechanism (Scheme 1). Weak dipole-dipole interactions between ^{129}Xe nuclear spins discount the possibility for through-space depolarization effects. However, there may be significant chemical shift anisotropy of the xenon atom(s) associated with TAAC, which would significantly accelerate relaxation of ^{129}Xe nuclei.[50,51] In addition, with induced electron currents in the bound Xe@TAAC complex,[52] meaningful variations of xenon local magnetic fields can be present, providing another depolarization pathway.[53] However, neither effect can explain the >10-fold discrepancy between k_{off} measured by NMR linewidth (all Xe isotopes) and the faster k_{cat} Xe depolarization rate determined by Hyper-CEST.

We surmise that the exchange rates that are measurable by either 1-D EXSY or NMR line widths are not measuring the pairwise Xe-Xe exchange rate, but instead a slower process involving the exchange of Xe for intermediary solvent in the ~20% of "empty" (water-bound) TAAC molecules. To consider the potential for a much faster Xe-Xe exchange process, we note the previous observation that Xe exchange rates for cryptophanes in organic solution are accelerated at higher Xe concentrations, indicating an "associative" exchange mechanism.[29] Direct Xe-Xe exchange may be critical for avoiding a solvent-bound "kinetic trap", which we propose should deactivate cryptophane for efficient Hyper-CEST.

Notably, 1.4 pM TAAC detection sensitivity was achieved with natural isotopic abundance Xe (26.4% ^{129}Xe) polarized to 10–15%. Thus, most of the TAAC host molecules in solution were occupied with other “silent” Xe isotopes or “thermally polarized” ^{129}Xe nuclei not contributing to bulk magnetization. At the initiation of the experiment, TAAC-bound HP ^{129}Xe concentration was estimated to be: [TAAC] × TAAC occupancy percentage × ^{129}Xe isotopic abundance × hyperpolarization level = 1.4 pM × 80% × 26.4% × 10% = 0.03 pM. Our analysis predicts that at least 10-fold greater detection sensitivity may be achieved for TAAC bound with more highly polarized (50%), isotopically-enriched (86%) ^{129}Xe—conditions that should allow more efficient depolarization of ^{129}Xe by RF pulses, ‘catalyzed’ by TAAC. In this way, femtomolar detection of TAAC and related xenon-binding molecules should be readily achievable.

CONCLUSIONS

Using ^{129}Xe Hyper-CEST NMR spectroscopy, we detected a water-soluble cryptophane TAAC at concentrations as low as 1.4 pM, through enhancement from fast chemical exchange. This is a uniquely sensitive NMR measurement, and, in particular, represents a roughly 100-fold improvement in detection sensitivity over recently published ^{129}Xe Hyper-CEST NMR data, on a per cryptophane basis.[15] To investigate the role of TAAC in improving detection sensitivity, Xe binding kinetics of TAAC were characterized for the first time, by combining exchange lifetime with association constant measurements. Favorable thermodynamic and kinetic properties of Xe binding to TAAC were determined.

Kinetic analysis of Hyper-CEST NMR experiments with TAAC revealed a rapid, TAAC-mediated ^{129}Xe depolarization mechanism (k_{TAAC}[HP ^{129}Xe] = 1.7 × 10^{-7} M·s^{-1}), which corresponds to 1.2 × 10^4 HP ^{129}Xe atoms depolarized per second. Assuming near unity saturation efficiency, this corresponds to greater than one order of magnitude faster Xe exchange than k_{off} measured by 1-D EXSY and linewidth NMR measurements, which we assign to HP ^{129}Xe exchanging with H_2O in the cryptophane cavity. The sub-millisecond kinetic process identified by Hyper-CEST NMR experiments at 320 K is consistent with efficient Xe-Xe exchange. Ongoing theoretical calculations and experiments using different cryptophane moieties are investigating the significance of these two possible Xe exchange pathways. In conclusion, ultrasensitive cryptophane detection supports the further development of xenon host molecules and cryptophane-based biosensors for in vitro and in vivo ^{129}Xe magnetic resonance studies.

Supplementary Material

Refer to Web version on PubMed Central for supplementary material.

Acknowledgments

We thank George Furst and Gu Jun for helping with NMR instrument setup. This work was supported by NIH R01 GM097478.

REFERENCES

1. Walker TG, Happer W. Rev. Mod. Phys. 1997; 69:629.
2. Ruset IC, Ketel S, Hersman FW. Phys. Rev. Lett. 2006; 96 053002.
3. Wei Q, Seward GK, Hill PA, Patton B, Dimitrov IE, Kuzma NN, Dmochowski IJ. J. Am. Chem. Soc. 2006; 128:13274. [PubMed: 17017809]
4. Hill PA, Wei Q, Eckenhoff RG, Dmochowski IJ. J. Am. Chem. Soc. 2007; 129:9262. [PubMed: 17616197]

5. Hill PA, Wei Q, Troxler T, Dmochowski IJ. J. Am. Chem. Soc. 2009; 131:3069. [PubMed: 19239271]
6. Jacobson DR, Khan NS, Collé R, Fitzgerald R, Laureano-Pérez L, Bai Y, Dmochowski IJ. Proc. Natl. Acad. Sci. U. S. A. 2011; 108:10969. [PubMed: 21690357]
7. Spence MM, Rubin SM, Dimitrov IE, Ruiz EJ, Wemmer DE, Pines A, Yao SQ, Tian F, Schultz PG. Proc. Natl. Acad. Sci. U. S. A. 2001; 98:10654. [PubMed: 11535830]
8. Schröder L, Lowery TJ, Hilty C, Wemmer DE, Pines A. Science. 2006; 314:446. [PubMed: 17053143]
9. Baumer D, Brunner E, Blümler P, Zänker PP, Spiess HW. Angew. Chem., Int. Edit. 2006; 45:7282.
10. Brotin T, Dutasta JP. Chem. Rev. 2009; 109:88. [PubMed: 19086781]
11. Driehuys B, Moller HE, Cleveland ZI, Pollaro J, Hedlund LW. Radiology. 2009; 252:386. [PubMed: 19703880]
12. Boutin C, Stopin A, Lenda F, Brotin T, Dutasta JP, Jamin N, Sanson A, Boulard Y, Leteurtre F, Huber G, Bogaert-Buchmann A, Tassali N, Desvaux H, Carrière M, Berthault P. Bioorg. Med. Chem. 2011; 19:4135. [PubMed: 21605977]
13. Boutin C, Desvaux H, Carrière M, Leteurtre F, Jamin N, Boulard Y, Berthault P. NMR Biomed. 2011; 24:1264. [PubMed: 22223364]
14. Zhou X, Graziani D, Pines A. Proc. Natl. Acad. Sci. U. S. A. 2009; 106:16903. [PubMed: 19805177]
15. Meldrum T, Seim KL, Bajaj VS, Palaniappan KK, Wu W, Francis MB, Wemmer DE, Pines A. J. Am. Chem. Soc. 2010; 132:5936. [PubMed: 20392049]
16. Schröder L. Phys. Medica. 2011 in press.
17. Xu X, Norquay G, Parnell SR, Deppe MH, Ajraoui S, Hashoian R, Marshall H, Griffiths PD, Parra-Robles J, Wild JM. Magnet. Reson. Med. 2012 In Press.
18. Mugler JP, Altes TA, Ruset IC, Dregely IM, Mata JF, Miller GW, Ketel S, Ketel J, Hersman FW, Ruppert K. Proc. Natl. Acad. Sci. U. S. A. 2010; 107:21707. [PubMed: 21098267]
19. Cheng CY, Stamatatos TC, Christou G, Bowers CR. J. Am. Chem. Soc. 2010; 132:5387. [PubMed: 20349986]
20. Kunth M, Döpfert J, Witte C, Rossella F, Schröder L. Angew. Chem., Int. Edit. 2012; 51:8217.
21. Happer W, Miron E, Schaefer S, Schreiber D, van Wijngaarden WA, Zeng X. Phys. Rev. A. 1984; 29:3092.
22. Taratula O, Dmochowski IJ. Curr. Opin. Chem. Biol. 2010; 14:97. [PubMed: 19914122]
23. Viale A, Aime S. Curr. Opin. Chem. Biol. 2010; 14:90. [PubMed: 19913452]
24. Hancu I, Dixon WT, Woods M, Vinogradov E, Sherry AD, Lenkinski RE. Acta Radiol. 2010; 51:910. [PubMed: 20828299]
25. Viswanathan S, Kovacs Z, Green KN, Ratnakar SJ, Sherry AD. Chem. Rev. 2010; 110:2960. [PubMed: 20397688]
26. Sherry AD, Woods M. Annu. Rev. Biomed. Eng. 2008; 10:391. [PubMed: 18647117]
27. Woods M, Woessner DE, Sherry AD. Chem. Soc. Rev. 2006; 35:500. [PubMed: 16729144]
28. Aime S, Castelli DD, Terreno E. Angew. Chem., Int. Edit. 2005; 44:5513.
29. Bartik K, Luhmer M, Dutasta JP, Collet A, Reisse J. J. Am. Chem. Soc. 1998; 120:784.
30. Fogarty HA, Berthault P, Brotin T, Huber G, Desvaux H, Dutasta JP. J. Am. Chem. Soc. 2007; 129:10332. [PubMed: 17676741]
31. Fairchild RM, Joseph AI, Holman KT, Fogarty HA, Brotin T, Dutasta JP, Boutin C, Huber G, Berthault P. J. Am. Chem. Soc. 2010; 132:15505. [PubMed: 20958059]
32. Traore T, Clave G, Delacour L, Kotera N, Renard PY, Romieu A, Berthault P, Boutin C, Tassali N, Rousseau B. Chem. Comm. 2011; 47:9702. [PubMed: 21792442]
33. Mynar JL, Lowery TJ, Wemmer DE, Pines A, Fréchet JMJ. J. Am. Chem. Soc. 2006; 128:6334. [PubMed: 16683795]
34. Roy V, Brotin T, Dutasta JP, Charles MH, Delair T, Mallet F, Huber G, Desvaux H, Boulard Y, Berthault P. ChemPhysChem. 2007; 8:2082. [PubMed: 17712828]

35. Chambers JM, Hill PA, Aaron JA, Han Z, Christianson DW, Kuzma NN, Dmochowski IJ. J. Am. Chem. Soc. 2009; 131:563. [PubMed: 19140795]
36. Schlundt A, Kilian W, Beyermann M, Sticht J, Gunther S, Hopner S, Falk K, Roetzschke O, Mitschang L, Freund C. Angew. Chem., Int. Edit. 2009; 48:4142.
37. Berthault P, Desvaux H, Wendlinger T, Gyejacquot M, Stopin A, Brotin T, Dutasta JP, Boulard Y. Chem. Eur. J. 2010; 16:12941. [PubMed: 20886471]
38. Meldrum T, Schröder L, Denger P, Wemmer DE, Pines A. J. Magn. Reson. 2010; 205:242. [PubMed: 20542715]
39. Seward GK, Bai Y, Khan NS, Dmochowski IJ. Chem. Sci. 2011; 2:1103.
40. Zook AL, Adhyaru BB, Bowers CR. J. Magn. Reson. 2002; 159:175. [PubMed: 12482697]
41. Brotin T, Lesage A, Emsley L, Collet A. J. Am. Chem. Soc. 2000; 122:1171.
42. Brotin T, Devic T, Lesage A, Emsley L, Collet A. Chem. Eur. J. 2001; 7:1561. [PubMed: 11330913]
43. Spence MM, Ruiz EJ, Rubin SM, Lowery TJ, Winssinger N, Schultz PG, Wemmer DE, Pines A. J. Am. Chem. Soc. 2004; 126:15287. [PubMed: 15548026]
44. Aski SN, Takacs Z, Kowalewski J. Magn. Reson. Chem. 2008; 46:1135. [PubMed: 18800339]
45. Clever, HL., editor. IUPAC Solubility Data Series, Vol. 2: Krypton, Xenon and Radon - Gas Solubilities. Pergamon Press; 1979.
46. Seward GK, Wei Q, Dmochowski IJ. Bioconjug. Chem. 2008; 19:2129. [PubMed: 18925770]
47. Taratula O, Hill PA, Khan NS, Carroll PJ, Dmochowski IJ. Nat. Commun. 2010; 1:148. [PubMed: 21266998]
48. Schröder L, Meldrum T, Smith M, Lowery TJ, Wemmer DE, Pines A. Phys. Rev. Lett. 2008; 100
49. Lowery TJ, Garcia S, Chavez L, Ruiz EJ, Wu T, Brotin T, Dutasta JP, King DS, Schultz PG, Pines A, Wemmer DE. ChemBioChem. 2006; 7:65. [PubMed: 16342304]
50. Brouwer DH, Alavi S, Ripmeester JA. Phys. Chem. Chem. Phys. 2007; 9:1093. [PubMed: 17311152]
51. Hanni M, Lantto P, Vaara J. Phys. Chem. Chem. Phys. 2011; 13:13704. [PubMed: 21709898]
52. Gomes JANF, Mallion RB. Chem. Rev. 2001; 101:1349. [PubMed: 11710225]
53. Forgeron MAM, Wasylishen RE, Penner GH. J. Phys. Chem. A. 2004; 108:4751.
54. Meldrum T, Bajaj VS, Wemmer DE, Pines A. J. Magn. Reson. 2011; 213:14. [PubMed: 21974996]

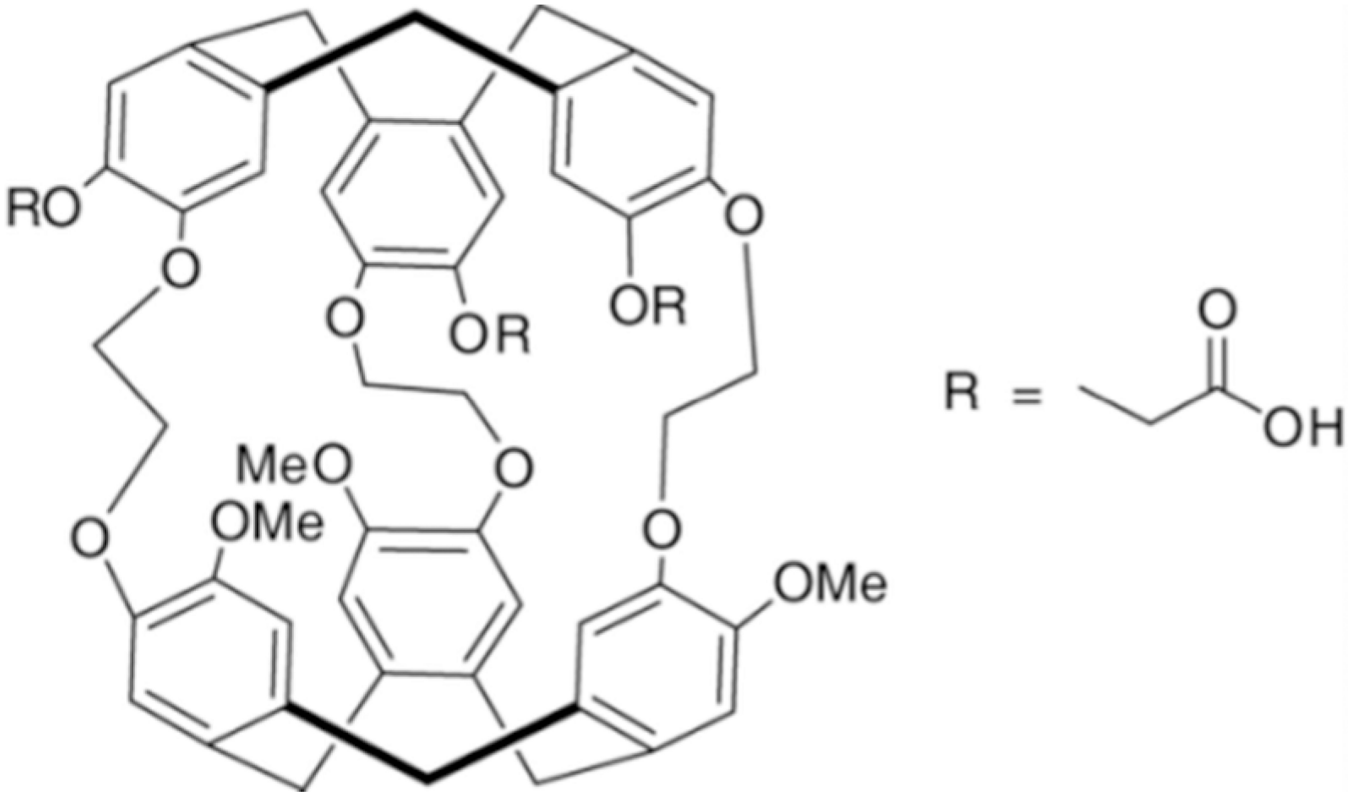

Figure 1.
Triacetic acid cryptophane-A derivative (TAAC).[5]

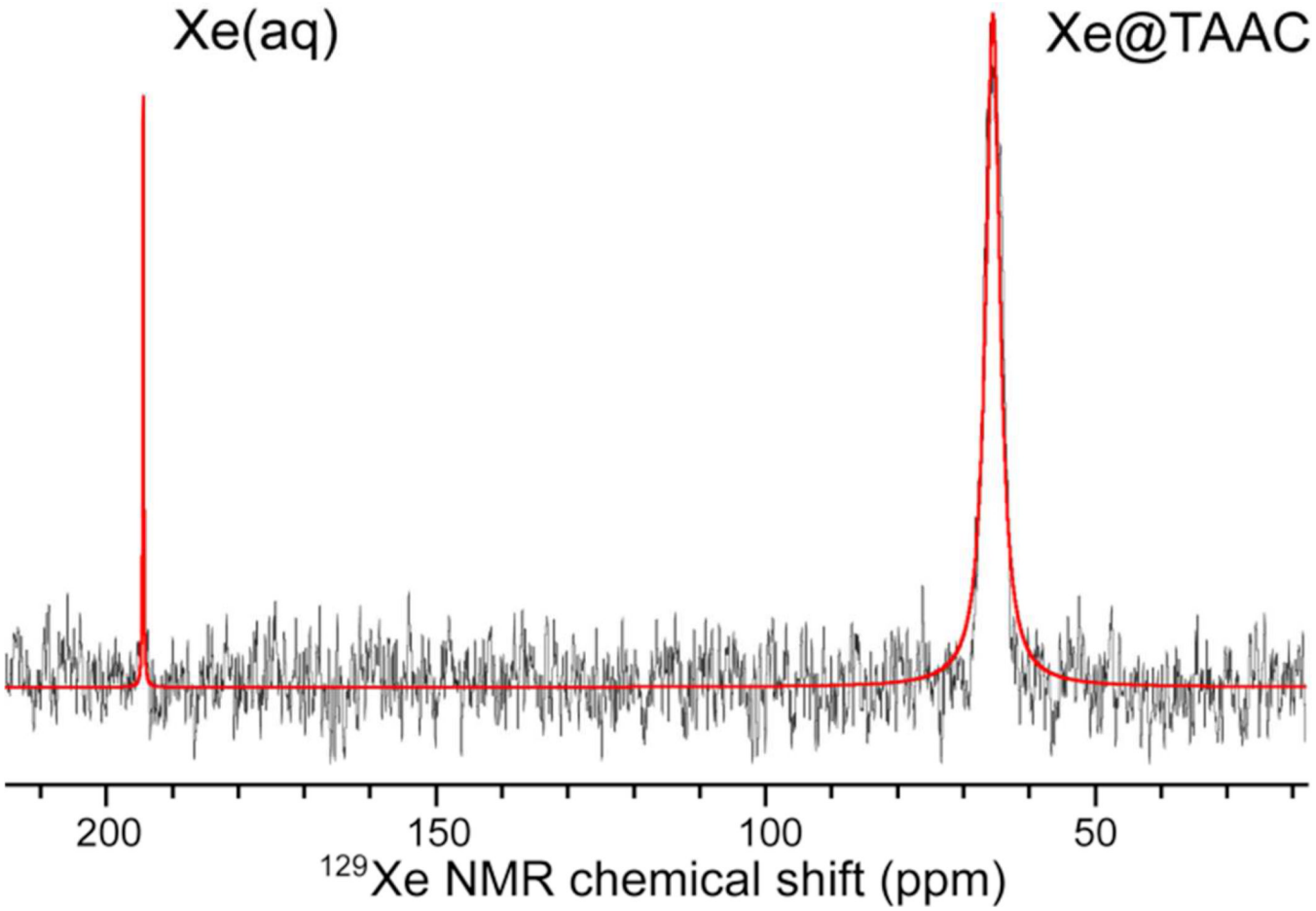

Figure 2.
HP ^{129}Xe NMR spectrum of 140 μM TAAC dissolved in ultrafiltered water at 320 K, showing: Xe(aq) peak at 194.3 ppm and Xe@TAAC peak at 65.8 ppm (selectively excited). Lorentzian deconvolved spectrum is shown in red.

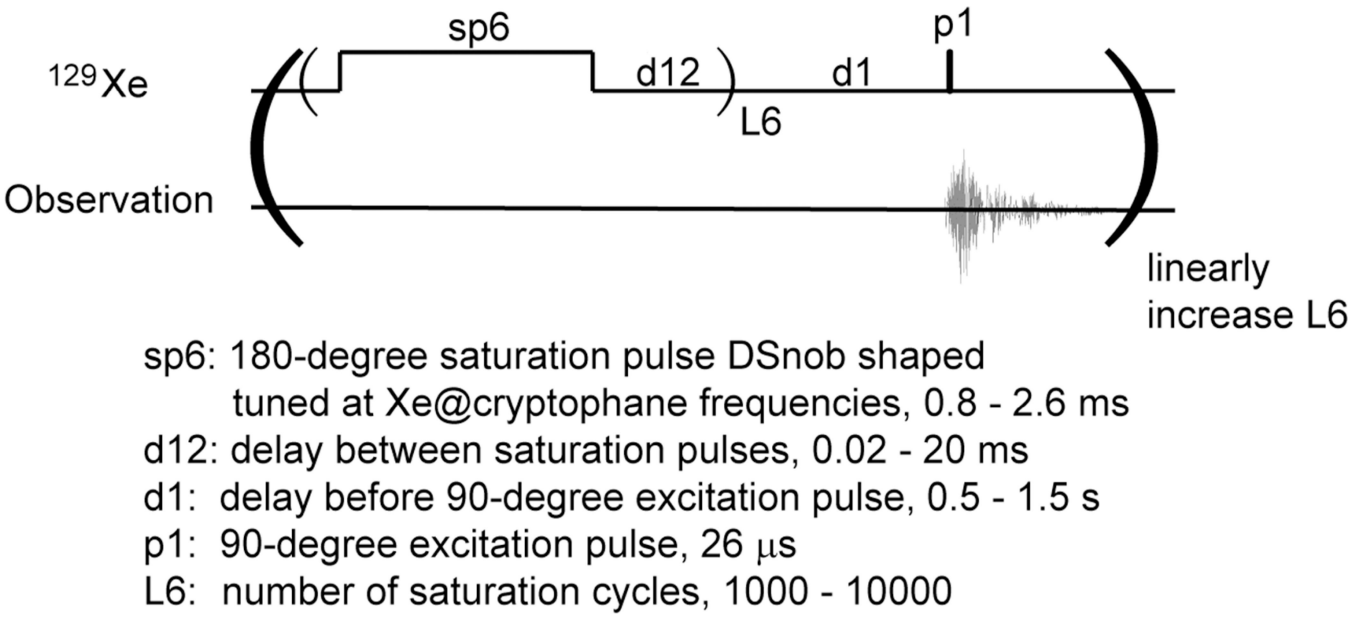

Figure 3.
Hyper-CEST pulse sequence diagram, with parameters provided for in-house 10 mm PABBO probe. Different values were chosen considering TAAC concentration, sample temperature, HP Xe flow rate. From a recent saturation transfer optimization,[54] saturation pulse is DSnob-shaped to enhance power efficiency. Field strength of the shaped pulse was calculated to be 29 μT (cw equivalent).

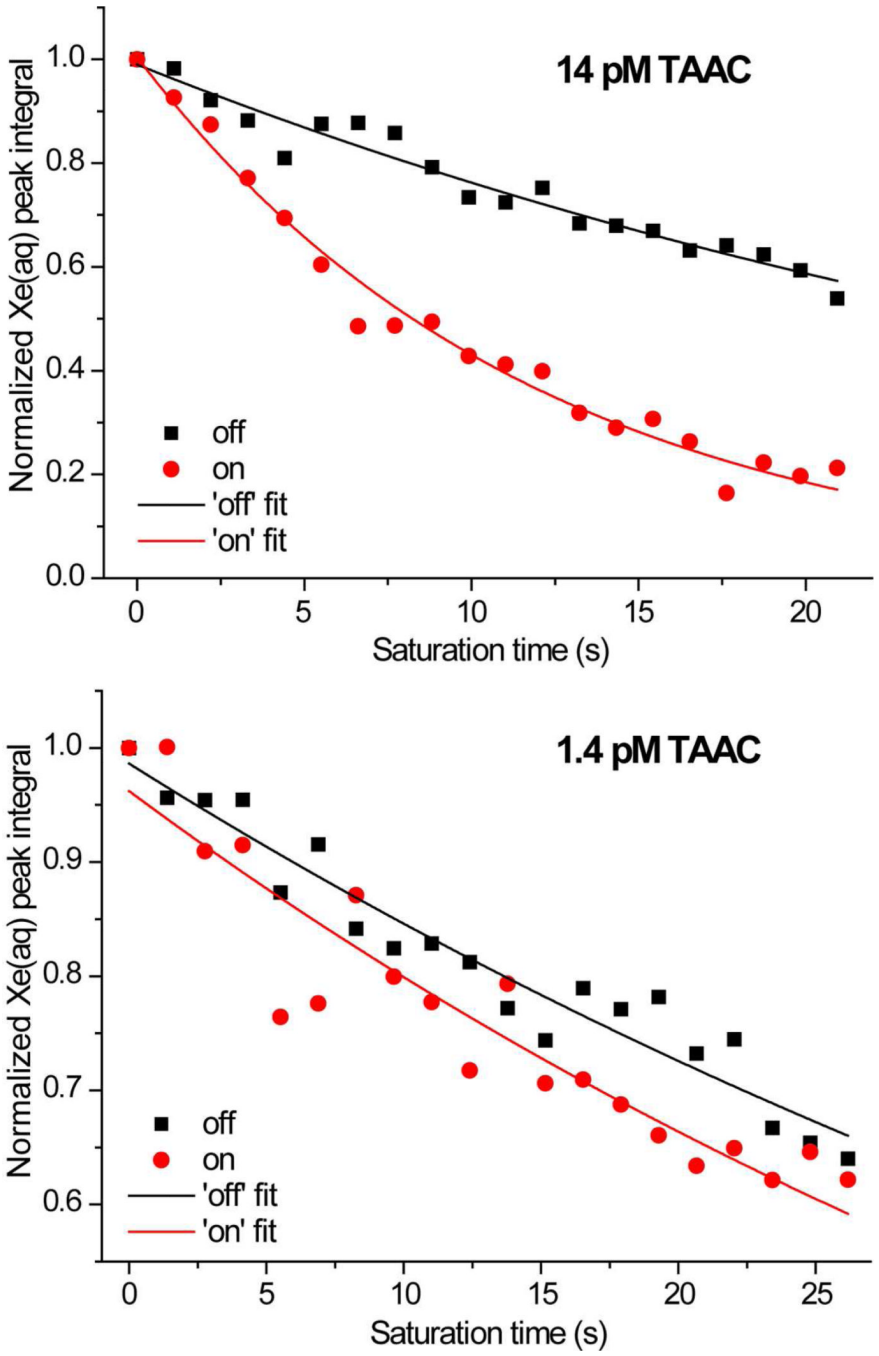

Figure 4.

^{129}Xe Hyper-CEST profiles of 14 pM and 1.4 pM TAAC at 320 K plotted as the Xe(aq) peak intensities vs. saturation time. Differences between on- and off-resonance saturation are compared. Exponential fits of data are shown as red and dark curves. Depolarization lifetimes were fitted to be 10 ± 1 s (on) and 38 ± 2 s (off) for 14 pM sample (averaged over two trials); 53 ± 4 s (on) and 65 ± 4 s (off) for 1.4 pM sample (representative of 3 trials), respectively. In each experiment, a series of 2.6 ms DSnob pulses with 20 μs delay was applied. In the Hyper-CEST pulse sequence, the following parameters were used: sp6 = 2.6 ms, d12 = 20 μs, d1 = 1 s, L6 = 8 000 (max, 14 pM) or 10 000 (max, 1.4 pM).

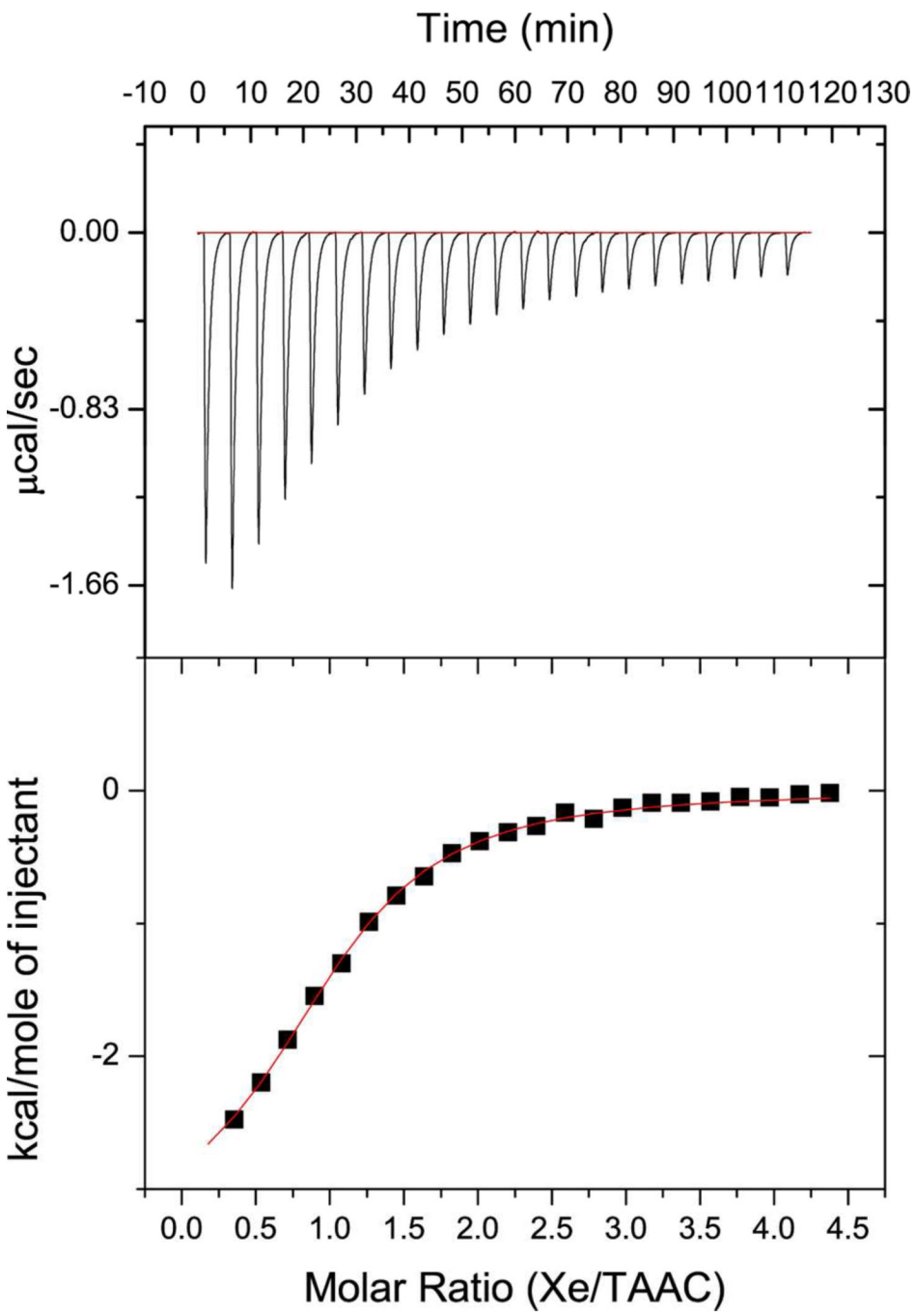

Figure 5.
Enthalpogram of 3.31 mM aqueous xenon solution[45] titrated into 131 µM TAAC solution (phosphate buffer, 20 mM, pH 7.5) at 310 K.

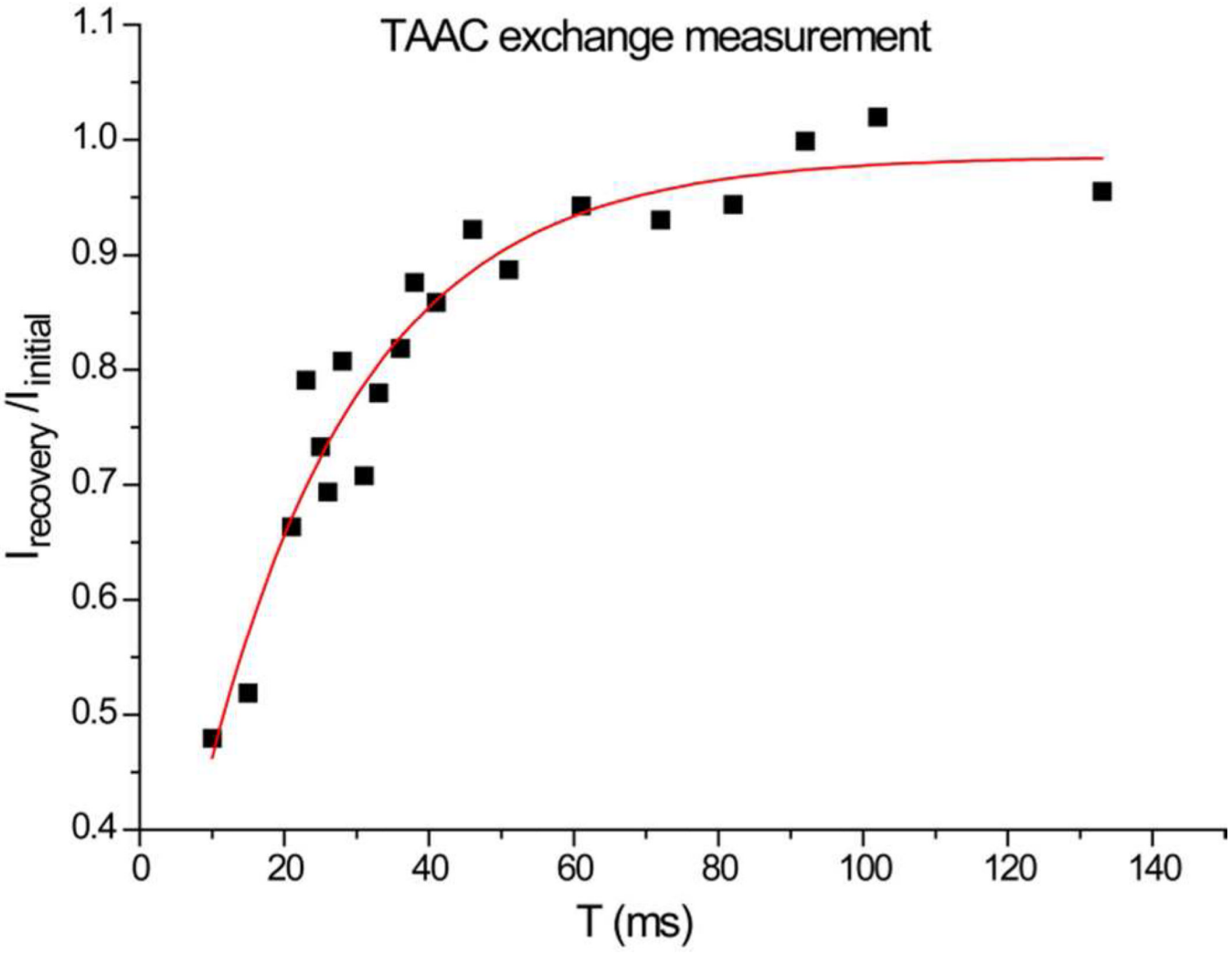

Figure 6.

Xe-TAAC exchange lifetime measurement by selective EXSY at 297 K. The horizontal axis denotes the mixing time between two consecutive excitations. The vertical axis indicates the ratio of the integrated intensities of Xe@TAAC signals, exchange recovered vs. equilibrium. Data were exponentially fitted to give an exchange lifetime, τ_{exch} = 22 ± 3 ms. This exchange lifetime is in good agreement with linewidth measurements made at 300 K (Table 1).

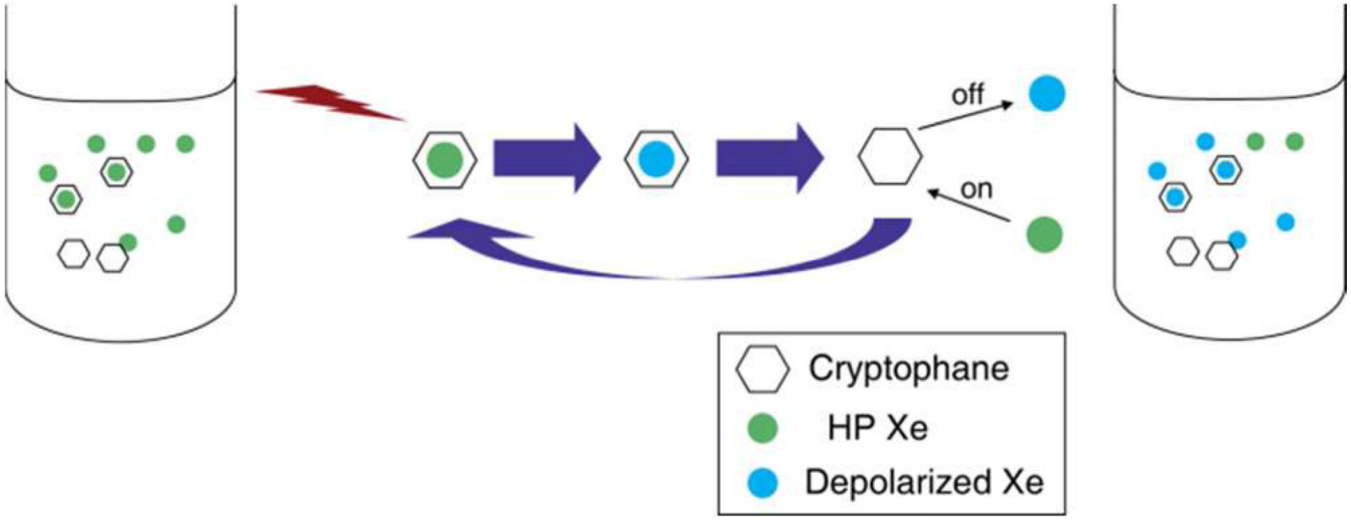

Scheme 1.
Saturation transfer processes in ^{129}Xe Hyper-CEST NMR with cryptophane.

Table 1

Line width of ^{129}Xe@TAAC NMR peak at various temperatures, and estimated Xe exchange rates.

Temperature (K)	Line width of Xe@TAAC peak (Hz)*	Estimated k_{exch} (s^{-1})
300	27.3 ± 1.1	86 ± 3.4
310	157.3 ± 1.1	500 ± 3.4
315	238.3± 3.6	750 ± 11
320	342.2 ± 5.7	1100 ± 18
325	294.2 ± 3.2	920 ± 10

* Magnetic homogeneity corrected.